Article

Validation of the corticomedullary difference in magnetic resonance imaging-derived apparent diffusion coefficient for kidney fibrosis detection: a cross-sectional study

BERCHTOLD, Lena, *et al*.

Abstract

Background: Kidney cortical interstitial fibrosis (IF) is highly predictive of renal prognosis and is currently assessed by the evaluation of a biopsy. Diffusion magnetic resonance imaging (MRI) is a promising tool to evaluate kidney fibrosis via the apparent diffusion coefficient (ADC), but suffers from inter-individual variability. We recently applied a novel MRI protocol to allow calculation of the corticomedullary ADC difference (ΔADC). We here present the validation of ΔADC for fibrosis assessment in a cohort of 164 patients undergoing biopsy and compare it with estimated glomerular filtration rate (eGFR) and other plasmatic parameters for the detection of fibrosis. Methods: This monocentric cross-sectional study included 164 patients undergoing renal biopsy at the Nephrology Department of the University Hospital of Geneva between October 2014 and May 2018. Patients underwent diffusion-weighted imaging, and T1 and T2 mappings, within 1 week after biopsy. MRI results were compared with gold standard histology for fibrosis assessment. Results: Absolute cortical ADC or cortical T1 values correlated poorly to IF [...]

Reference

BERCHTOLD, Lena, *et al*. Validation of the corticomedullary difference in magnetic resonance imaging-derived apparent diffusion coefficient for kidney fibrosis detection: a cross-sectional study. *Nephrology, Dialysis, Transplantation*, 2019

DOI : 10.1093/ndt/gfy389
PMID : 30608554

Original NDT

Validation of the cortico-medullary difference in MRI-derived apparent diffusion coefficient for kidney fibrosis detection: a cross-sectional study

Lena Berchtold*[1-2], Iris Friedli*[3], Lindsey A Crowe[3], Chantal Martinez[2], Solange Moll[4], Karine Hadaya[2], Thomas de Perrot[3], Christophe Combescure[5], Pierre-Yves Martin[2], Jean-Paul Vallée[3], Sophie de Seigneux**[2]**

***Equal contribution**

****** Equal contribution**

[1]Service of Internal Medicine, Department of Internal Medicine, University Hospital of Geneva, Geneva, Switzerland

[2]Service and Laboratory of Nephrology, Department of Internal Medicine Specialties and of Physiology and Metabolism, University and University Hospital of Geneva, Geneva, Switzerland.

[3]Service of Radiology, Department of Radiology and Medical Informatics, University Hospital of Geneva, Geneva, Switzerland.

[4]Institute of Clinical Pathology, Department of Clinical Pathology, University Hospital of Geneva, Geneva, Switzerland

[5]Division of clinical epidemiology, University Hospital of Geneva, Geneva, Switzerland

Running title: Diffusion MRI for fibrosis evaluation

Corresponding author:

Sophie de Seigneux

Service and Laboratory of Nephrology

4 rue Gabrielle-Perret-Gentil

1205 Geneva, Switzerland, email: sophie.deseigneux@hcuge.ch

Abstract:

Background: Kidney cortical interstitial fibrosis (IF) is highly predictive of renal prognosis, and is currently assessed by the evaluation of a biopsy. Diffusion MRI is a promising tool to evaluate kidney fibrosis via the apparent diffusion coefficient (ADC), but suffers from inter-individual variability. We recently applied a novel MRI protocol to allow calculation of the cortico-medullary ADC difference (ΔADC). We here present the validation of ΔADC for fibrosis assessment in a cohort of 164 patients undergoing biopsy and compare it to eGFR and other plasmatic parameters for the detection of fibrosis.

Methods: This monocentric cross-sectional study included 164 patients undergoing renal biopsy at the Nephrology Department of the University Hospital of Geneva between October 2014 and May 2018. Patients underwent diffusion-weighted imaging, and T1- and T2-mappings, within one week after biopsy. MRI results were compared to gold standard histology for fibrosis assessment.

Results: Absolute cortical ADC or cortical T1 values correlated poorly to IF assessed by the biopsy, whereas ΔADC was highly correlated to IF ($r=-0.52$, $p<0.001$) and eGFR ($r=0.37$, $p<0.01$), in both native and allograft patients. ΔT1 displayed a lower, but significant, correlation to IF and eGFR, whereas T2 did not correlate to IF nor to eGFR. ΔADC, ΔT1 and eGFR were independently associated with kidney fibrosis, and their combination allowed detecting extensive fibrosis with good specificity.

Conclusion: ΔADC is better correlated to IF than absolute cortical or medullary ADC values. ΔADC, ΔT1and eGFR are independently associated to IF and allow the identification of patients with extensive IF.

Keywords: MRI, fibrosis, diffusion, cortex, chronic kidney disease

Introduction:

Chronic kidney disease (CKD) is defined as abnormal kidney structure and/or function lasting for more than 3 months[1,2]. Whereas kidney function may be evaluated using creatinine and cystatin based equations, kidney structure is more difficult to appreciate non-invasively. The histological hallmark of CKD is the presence of cortical interstitial fibrosis (IF). IF is better correlated to renal function and to long term renal outcome than glomerulosclerosis or any other histological lesions[3,4]. Evaluation of IF is therefore used to tailor treatment and judge renal prognosis[5-7]. This evaluation is currently performed by the visual inspection of a kidney biopsy using specific stains such as Masson trichrome and/or Sirius Red[8]. Recent evidence has shown that the extent of interstitial fibrosis is one of the main factor predicting renal function evolution, even independently of eGFR[9].

In several organs, noninvasive ways to evaluate fibrosis are available. The kidney possesses specific features rendering it more difficult to image. It is a heterogeneous organ, and its global evaluation may be difficult[10]. In addition, native kidneys are located quite deep, move with respiration, and are close to air/tissue interfaces (intestines) limiting image quality and subsequent analysis. Non-invasive evaluation of fibrosis would be useful to avoid kidney biopsies in cases of extensive fibrosis, to follow the evolution of kidney disease non-invasively, and to identify patients at risk of CKD with still preserved renal function. Imaging would be complementary to eGFR estimation for the detection of early kidney lesions. Finally, imaging the whole kidney may also point to the presence of scars that may be missed or, conversely, overrepresented by a biopsy.

Diffusion Weighted Magnetic resonance imaging (DW-MRI) has been described as promising for evaluation of renal fibrosis, since it may easily be performed on clinical scanners[11-13]. In both human disease and experimental kidney disease models, DW-MRI could identify diseased

versus healthy kidneys[11,14-21]. In experimental models, the apparent Diffusion Coefficient (ADC) derived from DW-MRI showed a good negative correlation to fibrosis[22,23]. In human kidneys, Inoue et al. showed that diffusion MRI was correlated to renal function and to IF in 37 diabetic patients having undergone biopsy[11]. In another study, ADC correlated to cortical IF and eGFR in 25 patients[12]. Although promising, diffusion MRI of abdominal organs is still difficult to use clinically because of the artifacts associated with image acquisition, as well as the inter-individual variations of the absolute ADC values[24]. Finally, although correlation to IF is observed, the additional role of perfusion in these associations is debated[25].

Given the limitations described above, we recently adapted renal diffusion with the application of a readout-segmented echo planar (EPI) sequence (RESOLVE)[26]. In healthy volunteers, we could demonstrate that this diffusion sequence led to better discrimination between the cortical and medullary parts of the kidney[26]. The use of the cortico-medullary ADC difference (ΔADC) reduced inter-individual variation, allowing for better comparison between subjects[26]. In a pilot study, ΔADC was very well correlated to fibrosis assessed by standard histology in 29 kidney allograft patients having undergone kidney biopsy[27].

We aimed here to perform an external validation of ΔADC for IF detection in a larger and mixed population of patients having undergone biopsy, using a different scanner to the pilot study. We performed a multivariable analysis to improve IF detection. We investigated the identification of patients with extensive fibrosis in this cohort.

Methods

Patients

We designed a cross-sectional study, including adult kidney allograft recipients and CKD patients who were planned for a kidney biopsy for clinical purposes. MRI was scheduled on the

same day as the biopsy whenever possible, or within one week. Patients, 18 years of age or older, who were followed at the University Hospital of Geneva, were eligible for enrollment. Exclusion criteria were the presence of a pacemaker or other MR incompatible device, pregnancy, claustrophobia, and patient refusal. In all patients, additional fasting serum and urine were collected and stored at -80℃. The study was approved by the local ethical committee for human studies of Geneva, Switzerland (CER 11-160, Commission Cantonale d'Ethique de la Recherche) and performed according to the Declaration of Helsinki principles. All the patients were contacted to provide written informed consent to participate in this prospective study. None of the patients were from a vulnerable population and all patients or next of kin provided written informed consent which was freely given.

Laboratory measurement

Baseline characteristics, including medical history, co-morbidities and treatment, were collected through patient records. Patients' blood pressure, weight and size were measured routinely during follow-up visits. Serum creatinine and other standard laboratory values were measured during routine follow-up visits or hospitalizations. Standard biochemical analyses were performed in a Geneva University Hospital Laboratory using routine automated analyzers. The eGFR was calculated using the Chronic Kidney Disease Epidemiology Collaboration equation (CKD-EPI). Creatinine was measured by Jaffé-kinetics using IDMS-traceable methods.

Histological fibrosis quantification

Renal fibrosis was assessed quantitatively on the kidney biopsy specimen by the Pathology Department of the University Hospital of Geneva, using Masson trichrome stained kidney sections. The expert pathologist (S.M.) was blinded to the other results, including eGFR and MRI. Expert evaluation of fibrosis is recommended to evaluate IF and is reproducible. It is the

current gold standard in most pathology services[9,28]. The severity of renal fibrosis was scored from 0 to 100% for each patient and reported on the clinical biopsy report independently of our study. To verify the reproducibility of this evaluation, 60 random sections were evaluated blindly by two experienced nephrologists. This repeated fibrosis evaluation displayed a good correlation to pathological evaluation (ICC 0.92; 95%CI 0.87 to 0.95). Furthermore, renal fibrosis was quantified using the BANFF criteria in renal allograft patients: ci (interstitial fibrosis) and ct (tubular atrophy) with a minimal score of 0 and maximal score of 6. Due to a good correlation between the two methods ($r = 0.86$; $p < 0.001$), we used subjective histological renal fibrosis as a continuous variable (0 to 100%) for all analyses. In our predictive models, we also use the fibrosis in categories (<10; 10-25; 25-50; >50 %) in both native and allograft patients, as recently proposed for renal prognosis[9].

MR imaging

Patients were scanned on a PRISMA 3T MR (Siemens AG, Erlangen Germany) with the standard 32-element spine coil and the 18-element phased-array abdominal coil. MRI protocol parameters are summarized in Table 1. ROI were determined as previously described[26,27] for diffusion-weighted ADC, T1 and T2 mapping, and the cortico-medullary differences were calculated. ADC was measured directly on the ADC map produced by the Siemens MR system, which uses a monoexponential fitting model. The analysis of the MRI images was also blinded to all other markers. The MRI was performed in 55% of the cases before the biopsy. In the remaining patients the biopsy was performed one week before MRI. All focal pathological areas (cyst, scar, hematomas …) were avoided in the ROI placement aiming to cover a large and representative part of the cortex and medulla.

Statistical analysis

Continuous variables are expressed as mean ± standard deviation or median and interquartile range according to the distribution. Categorical variables are expressed as numbers and percentages. The statistical significance was determined as a p value of less than 0.05 and all tests were two-sided. For simple correlation analyses, we performed Pearson's tests, after controlling the linearity of associations with scatterplots. We conducted univariable and multivariable linear regression analyses to assess the associations with IF[29]. Univariable and multivariable logistic regression models were used to investigate the capacity of parameter to predict different levels of fibrosis and vascular lesions. The discriminative performance of markers and logistic regression models to predict different levels of fibrosis and vascular lesions were assessed by using receiver operating characteristic (ROC) curves. We reported AUC values with 95%CI. Statistical analyses were performed using STATA 13.1 (StataCorp, College Station, TX, USA).

Results:

Characteristics of the study population

From October 2014 to May 2018, we included 164 CKD patients, mainly Caucasian (91%) and male (67%), undergoing kidney biopsy for clinical reasons. Of the 164 patients, 118 (72%) were kidney allograft patients and 46 (28%) were native kidney patients (Figure 1). Baseline characteristics are presented in Table 2. Biopsy indications were made by the nephrologist in charge of the patients, as clinically justified, and independently of the present study. For native kidney disease, most of the indications were an abnormal urinary microscopy and proteinuria and/or acute or chronic renal dysfunction. For allograft patients, biopsy indications were routine biopsies (at one year, after steroid withdrawal), elevation of creatinine levels, and apparition of proteinuria or de novo donor specific antibodies.

Univariable analysis of predictors of fibrosis

MRI indexes for IF evaluation: ΔADC, ΔT1 and ΔT2

Images for 97% of the patients were of sufficient quality to allow measurement of the difference between ADC of the cortex and medulla (ΔADC values [x10−6mm2/s]) (Figure 2). In order to validate ΔADC for IF evaluation in this population, we correlated ΔADC with IF assessed by the gold standard clinical IF evaluation method. We confirmed a statistically significant and high correlation between these parameters ($r = -0.52$, $p<0.001$) (Figure 3A). Absolute cortical ADC values correlated moderately to IF ($r = -0.22$, $p = 0.01$), whereas medullary ADC did not correlate with IF (Supplementary 1A-B). The correlation of ΔADC to IF was stronger in native kidney patients ($r=-0.64$, $p<0.001$) than in kidney allograft patients ($r= -0.42$, $p<0.001$) (Supplementary Figure 2). ΔADC correlated to eGFR ($r=0.37$, $p <0.001$) (Figure 1C).

In patients with relatively preserved normal renal function (eGFR ≥60ml/min), ΔADC still correlated to IF (r=-0.27, p=0.03), whereas the correlation was even stronger in patients with eGFR <60ml/min/1.73m^2 (r= -0.53, p<0.01). Cortical and medullary ADC values did not correlate to IF in patients with eGFR≥60 ml/min/1.73m^2, and the correlations were not statistically significant, with a limit p-value, in patients with an eGFR lower than 60 ml/min/1.73 m^2. Cortical and medullary ADC did not correlate significantly to eGFR ((r = 0.15, p=0.07) and (r=-0.04, p=0.58) respectively).

A moderate correlation was found between absolute T1 values and IF with r= 0.26, p = 0.005 for the cortex (Supplementary Figure 1C). Medullary T1 was inversely correlated to IF r = -0.20, p= 0.03 (Supplementary Figure 1D). We further calculated the cortico-medullary difference for T1 values (ΔT1). ΔT1 displayed a better correlation to IF (r = 0.49, p < 0.001) than absolute values (Figure 3B). The correlation between IF and ΔT1 was stronger in native kidney patients than in kidney allograft patients (supplementary Figure 2). Cortical and medullary T1 did not correlate with eGFR (r=-0.13, p=0.09 and r=0.15, p=0.06 respectively) whereas ΔT1 did (r = -0.30, p < 0.001) (Figure 3D).

Neither T2 nor ΔT2 correlated with renal function nor with IF, in both native kidney and kidney allograft patients (Supplementary Figure 3).

Biological parameters

In order to test whether combining plasmatic and MRI variables could improve the detection of fibrosis, we tested the association between fibrosis and different biological parameters in univariable analysis (Supplementary Figure 4). Parameters eGFR, PTH, 25-OH vitamin D, proteinuria, phosphate and hemoglobin displayed good correlation to IF as shown in Table 3.

Multivariable model.

In the complete multivariable analysis presented in Table 3, only ΔT1, ΔADC and eGFR were independently associated with fibrosis.

The coefficient R^2 of the complete multivariable model was 0.54 (R=0.74) (Table 3), indicating that the combination of parameters improved the detection of IF. No significant interaction was observed between ΔT1, ΔADC and eGFR. Using the multivariable model, the higher the fibrosis category, the higher our predictive score (Figure 4).

When considering only the three independently associated factors (ΔADC, ΔT1, eGFR), the R^2 was also 0.54.

Identifications of patients by fibrosis categories

With a logistic model aiming to identify patients with low fibrosis (10% or less), the obtained combination of ΔADC, ΔT1 and eGFR showed an AUC of 0.840 (Figure 5A). 89 patients had a high level of risk to have a fibrosis predicted by the model greater than 10%, among which 85 had actual biopsy-measured fibrosis >10% (positive predictive value, PPV=95.5%). However, thresholds clinically relevant to rule-out patients with low fibrosis (i.e. thresholds with a high sensitivity) identified only a small subgroup of patients.

With a logistic model aiming to identify patients with a significant fibrosis (more than 25%), the AUC was 0.840 (Figure 5B). 18 patients were identified by the model with a low level of risk to have a fibrosis greater than 25%, among which 16 had actual biopsy-measured fibrosis <= 25% (negative predictive value, NPV=88.9%). 41 patients were identified by the model with a high level of risk to have a fibrosis greater than 25%, among which 37 had actual biopsy-measured fibrosis > 25% (PPV=86.3%).

With a logistic model aiming to identify patients with a significant fibrosis (50% or more), the AUC was 0.905 (Figure 5C). 127 patients were identified by the model with a low level of risk

to have a fibrosis of 50% or more, among which 127 had actual biopsy-measured fibrosis < 50% (NPV=96.2%). 9 patients were identified by the model with a high level of risk to have a fibrosis of 50% or more, among which 8 had actual biopsy-measured fibrosis >= 50% (PPV=88.8%). The ROC curves using the same threshold, but with only ΔADC as predictor, are represented in Supplementary Figure 5.

Discussion:

In this study, we externally validated an improved diffusion MRI sequence allowing the calculation of the cortico-medullary ADC difference for fibrosis detection in a mixed population of 164 patients who had undergone kidney biopsy for clinical purposes. We showed also ΔADC's superiority to absolute cortical ADC values. We used a different scanner than in our previous studies. We demonstrated that MRI parameters add to eGFR for IF detection. Finally, we showed that MRI parameters combined to eGFR identify patients with extensive fibrosis with a good specificity.

Although several studies have used diffusion MRI as a tool to evaluate fibrosis, differences between sequences and ADC values precluded clear comparison[30]. Our study represents, to the best of our knowledge, the largest study validating diffusion MRI to predict fibrosis in patients undergoing biopsies. The difference in cortical and medullary ADC correlated well to fibrosis in our mixed population of native and allograft kidneys, with various types of primary diseases, therefore validating our previous observation in a small homogeneous population. In addition, the difference index was stable between different brands and types of scanner (Friedli, ISMRM, 2017, abstract#3298). Diffusion MRI also did not require the use of contrast medium, an advantage in the CKD population. Interestingly, ΔADC correlated to fibrosis even with patients with preserved renal function, which may indicate that early detection of lesions is possible. Absolute ADC values were less correlated to fibrosis than ΔADC. Fibrosis usually affects the

cortex. Normalization to the medulla was technically easier and more efficient than to surrounding tissues outside the kidney, since the close proximity of the medulla decreased errors related to B1 and B0 heterogeneity as well as to the coil sensitivity profile [27]. Since medullary ADC was not correlated to fibrosis, subtracting it from the cortical ADC improved reproducibility and likely corrected for the baseline physiological inter-individual variability of the ADC[27]. The lower correlation between absolute ADC values and fibrosis compared to the existing literature is probably related to the mixed population we included, and this therefore calls for normalization of absolute cortical ADC values as an important tool in this research. We used here monoexponential fit for ADC calculation with all the b-values and not biexponential fit since we previously demonstrated that parameters derived from the biexponential fit did not improve detection of IF[31]. As perfusion may also be reduced in case of IF, we still believe that the whole range of b-values is useful for IF detection. As emphasized by a recent review[32], the monoexponential model is still preferred by the majority of studies on renal diffusion as the superiority of biexponential model in renal diffusion remains to be better demonstrated.

Fibrosis evaluation was more accurate in native kidney patients, which may be related to the lower number of patients in this group. Alternatively, the vasoconstriction usually observed in allograft patients, related to the use of calcineurin inhibitors, may modulate perfusion and affect diffusion MRI independently of fibrosis, lowering the association to fibrosis.

T1 mapping measures the longitudinal (spin-lattice) relaxation time and has been used to evaluate cardiac fibrosis[33]. We showed here that T1, in particular ΔT1, were also associated to renal IF, although not as strongly as ΔADC. Interestingly, the combination of ΔT1 and ΔADC in multivariable analysis improved fibrosis detection by imaging variables alone, showing that the two values measure slightly different phenomena. These two parameters may thus be complementary to predict fibrosis in the kidney.

We further demonstrated that adding ΔADC values to eGFR improves the correlation in a multivariable model suggesting that ΔADC and eGFR measure different parameters associated to IF, and are thus complementary. Whether ΔADC and ADC measure structural parameters or modifications of water movement of filtrate is much debated and difficult to demonstrate, but we showed here that diffusion correlated to IF, at least independently of glomerular filtration rate. Modifications of ADC may still be influenced by perfusion and other parameters that were not measured here. The important question of the origin of ADC change induced by IF remains to be addressed by further studies. In this respect, diffusion tensor imaging (DTI) that can assess the renal anisotropy may bring new insights[15,17,34]. Nevertheless, our aim was to evaluate ΔADC as an independent marker of IF, whatever the primary cause of the modification in signal.

Categories of IF have recently been demonstrated to predict renal function evolution[9]. We studied the value of MRI parameters in combination to eGFR to identify patients in four fibrosis categories. Our model was able to identify patients with more than 10% fibrosis with a great sensitivity, corresponding to early detection of structural lesions in relatively healthy kidneys. Our model could identify patients with extensive (>50%) IF with a good specificity. Although not perfect, addition of MRI to clinical evaluation may thus avoid biopsies or unnecessary treatment in selected cases, or could help tailor follow-up.

One limitation of our study is its monocentric design, despite the large number of patients included. Another source of error could be related to manual, therefore subjective, placement of ROIs. This procedure is still standard in the field of diffusion MRI and we have shown, in a previous study that our methodology had a good inter and intra-observer reproducibility[27]. We used the evaluation of a biopsy by a pathologist blinded for eGFR as gold standard for IF evaluation. To secure our evaluation, we performed a blinded second reading of the IF in 60 sections chosen randomly by two nephrologists. The agreement between the second reading and the pathologist reading was good (ICC: 0.92; 95%CI 0.87 to 0.95). Although automatic

kidney biopsy evaluation has been suggested to be useful in fibrosis estimation, it is still rarely performed routinely and correlated less well to eGFR than pathological evaluation[8] in this study population. This is likely because of the non-exclusion of glomeruli and vessels in these automatized quantifications (data not shown). We however observed a relatively good correlation between the pathological and automated evaluation of IF ($r=0.4$, $p<0.01$). Finally, subjective assessment of tubulo-interstitial fibrosis has been shown to have very high inter-reader agreement and is the current gold standard for IF assessment in pathology services[9,28]. Given these limitations, novel, more objective tools to quantify fibrosis are being developed, but are not routinely available[35,36]. Sampling error may also occur in random biopsies. This last limitation is however inherent to kidney biopsies. Finally, given the design of our study and the need to have MRI performed on a research timetable, we could not include many emergency biopsies and our population principally represents semi-elective biopsies (planned within one week) in native kidney and kidney allograft patients.

Overall, we externally validated the ΔADC as an excellent index to evaluate cortical fibrosis non-invasively, with much better accuracy than absolute cortical or medullary ADC values. We show that ΔADC is strongly associated to IF in both native and allograft patients. We further show that ΔADC may be used in combination with ΔT1 and eGFR to evaluate fibrosis, and that MRI parameters significantly improve the detection to IF. Finally, we show that our model is able to identify patients with extensive fibrosis with good specificity. Further studies on the prognostic value and the longitudinal follow-up of patients would be of interest.

Disclosures:

The authors have nothing to disclose

Acknowledgments

This work was supported by grants from the Clinical Research Center of the Medicine Faculty of Geneva University and Geneva University hospital, as well as the Leenards and Louis-Jeantet foundations and the Swiss National Foundation (JPV grant 320038_159714 and SDS grant PP00P3_127454). This work was supported in part by the Centre for Biomedical Imaging (CIBM) of EPFL, University of Geneva and the University Hospitals of Geneva and Lausanne and the Swiss National Foundation for its financial support for the PRISMA MRI (R'Equip grants: SNF No 326030_150816).

Authors's contributions:

SdS, LB, JPV, IF: study design, data acquisition, statistical analysis, manuscript writing, LC, TdP: data acquisition, manuscript writing, PYM: study design, manuscript revision, CM: data acquisition, SM: data acquisition, manuscript revision, KH: manuscript revision, CC: statistical analysis, manuscript revision

References

1. Levey, A.S. & Coresh, J. Chronic kidney disease. *Lancet* **379**, 165-180 (2012).
2. Levey, A.S*., et al.* The definition, classification and prognosis of chronic kidney disease: a KDIGO Controversies Conference report. *Kidney Int* (2010).
3. Eknoyan, G., McDonald, M.A., Appel, D. & Truong, L.D. Chronic tubulo-interstitial nephritis: correlation between structural and functional findings. *Kidney Int* **38**, 736-743 (1990).
4. Schainuck, L.I., Striker, G.E., Cutler, R.E. & Benditt, E.P. Structural-functional correlations in renal disease. II. The correlations. *Hum Pathol* **1**, 631-641 (1970).
5. Park, W.D., Griffin, M.D., Cornell, L.D., Cosio, F.G. & Stegall, M.D. Fibrosis with inflammation at one year predicts transplant functional decline. *J Am Soc Nephrol* **21**, 1987-1997 (2010).
6. Rush, D.N*., et al.* Factors associated with progression of interstitial fibrosis in renal transplant patients receiving tacrolimus and mycophenolate mofetil. *Transplantation* **88**, 897-903 (2009).
7. Barbour, S.J*., et al.* The MEST score provides earlier risk prediction in lgA nephropathy. *Kidney Int* **89**, 167-175 (2016).
8. Farris, A.B*., et al.* Morphometric and visual evaluation of fibrosis in renal biopsies. *J Am Soc Nephrol* **22**, 176-186 (2011).
9. Srivastava, A*., et al.* The Prognostic Value of Histopathologic Lesions in Native Kidney Biopsy Specimens: Results from the Boston Kidney Biopsy Cohort Study. *J Am Soc Nephrol* (2018).
10. Correas, J.M*., et al.* Ultrasound-based imaging methods of the kidney-recent developments. *Kidney Int* **90**, 1199-1210 (2016).
11. Inoue, T*., et al.* Noninvasive Evaluation of Kidney Hypoxia and Fibrosis Using Magnetic Resonance Imaging. *J Am Soc Nephrol* (2011).
12. Zhao, J*., et al.* Assessment of renal fibrosis in chronic kidney disease using diffusion-weighted MRI. *Clinical radiology* **69**, 1117-1122 (2014).
13. Leung, G*., et al.* Could MRI Be Used To Image Kidney Fibrosis? A Review of Recent Advances and Remaining Barriers. *Clin J Am Soc Nephrol* **12**, 1019-1028 (2017).
14. Cakmak, P., Yagci, A.B., Dursun, B., Herek, D. & Fenkci, S.M. Renal diffusion-weighted imaging in diabetic nephropathy: correlation with clinical stages of disease. *Diagnostic and interventional radiology* **20**, 374-378 (2014).
15. Feng, Q., Ma, Z., Wu, J. & Fang, W. DTI for the assessment of disease stage in patients with glomerulonephritis--correlation with renal histology. *Eur Radiol* **25**, 92-98 (2015).
16. Lanzman, R.S*., et al.* Kidney transplant: functional assessment with diffusion-tensor MR imaging at 3T. *Radiology* **266**, 218-225 (2013).
17. Liu, Z*., et al.* Chronic kidney disease: pathological and functional assessment with diffusion tensor imaging at 3T MR. *Eur Radiol* **25**, 652-660 (2015).
18. Lu, L*., et al.* Use of diffusion tensor MRI to identify early changes in diabetic nephropathy. *Am J Nephrol* **34**, 476-482 (2011).
19. Namimoto, T*., et al.* Measurement of the apparent diffusion coefficient in diffuse renal disease by diffusion-weighted echo-planar MR imaging. *Journal of magnetic resonance imaging : JMRI* **9**, 832-837 (1999).
20. Ries, M*., et al.* Renal diffusion and BOLD MRI in experimental diabetic nephropathy. Blood oxygen level-dependent. *Journal of magnetic resonance imaging : JMRI* **17**, 104-113 (2003).
21. Thoeny, H.C., De Keyzer, F., Oyen, R.H. & Peeters, R.R. Diffusion-weighted MR imaging of kidneys in healthy volunteers and patients with parenchymal diseases: initial experience. *Radiology* **235**, 911-917 (2005).

22. Togao, O*., et al.* Assessment of renal fibrosis with diffusion-weighted MR imaging: study with murine model of unilateral ureteral obstruction. *Radiology* **255**, 772-780 (2010).
23. Haque, M.E*., et al.* Longitudinal changes in MRI markers in a reversible unilateral ureteral obstruction mouse model: preliminary experience. *Journal of magnetic resonance imaging : JMRI* **39**, 835-841 (2014).
24. Le Bihan, D., Poupon, C., Amadon, A. & Lethimonnier, F. Artifacts and pitfalls in diffusion MRI. *Journal of magnetic resonance imaging : JMRI* **24**, 478-488 (2006).
25. Boor, P*., et al.* Diffusion-weighted MRI does not reflect kidney fibrosis in a rat model of fibrosis. *Journal of magnetic resonance imaging : JMRI* **42**, 990-998 (2015).
26. Friedli, I*., et al.* Improvement of renal diffusion-weighted magnetic resonance imaging with readout-segmented echo-planar imaging at 3T. *Magnetic resonance imaging* (2015).
27. Friedli, I*., et al.* New Magnetic Resonance Imaging Index for Renal Fibrosis Assessment: A Comparison between Diffusion-Weighted Imaging and T1 Mapping with Histological Validation. *Scientific reports* **6**, 30088 (2016).
28. Mariani, L.H*., et al.* Interstitial fibrosis scored on whole-slide digital imaging of kidney biopsies is a predictor of outcome in proteinuric glomerulopathies. *Nephrol Dial Transplant* **33**, 310-318 (2018).
29. Hidalgo, B. & Goodman, M. Multivariate or multivariable regression? *American journal of public health* **103**, 39-40 (2013).
30. Morrell, G.R., Zhang, J.L. & Lee, V.S. Magnetic Resonance Imaging of the Fibrotic Kidney. *J Am Soc Nephrol* **28**, 2564-2570 (2017).
31. Friedli, I*., et al.* Comparison of readout-segmented and conventional single-shot for echo-planar diffusion-weighted imaging in the assessment of kidney interstitial fibrosis. *Journal of magnetic resonance imaging : JMRI* **46**, 1631-1640 (2017).
32. Caroli, A*., et al.* Diffusion-weighted magnetic resonance imaging to assess diffuse renal pathology: a systematic review and statement paper. *Nephrol Dial Transplant* **33**, ii29-ii40 (2018).
33. Perea, R.J*., et al.* T1 mapping: characterisation of myocardial interstitial space. *Insights into imaging* **6**, 189-202 (2015).
34. Gaudiano, C*., et al.* Diffusion tensor imaging and tractography of the kidneys: assessment of chronic parenchymal diseases. *European radiology* **23**, 1678-1685 (2013).
35. Vuiblet, V*., et al.* Renal Graft Fibrosis and Inflammation Quantification by an Automated Fourier-Transform Infrared Imaging Technique. *J Am Soc Nephrol* **27**, 2382-2391 (2016).
36. Meas-Yedid, V*., et al.* New computerized color image analysis for the quantification of interstitial fibrosis in renal transplantation. *Transplantation* **92**, 890-899 (2011).

Table 1: MRI parameters used in this study

DWI: diffusion weighted imaging; T1: Longitudinal (spin-lattice) relaxation time; T2: Transverse (spin-spin) relaxation time, RESOLVE: Readout Segmentation of Long Variable Echo Trains; MOLLI: Modified Look-Locker Inversion-recovery; ADC: apparent diffusion coefficient

	RESOLVE DWI (for ADC)	**MOLLI T1 mapping**	**T2**
Resolution [mm^3]	**2×2×5**	**2×2×5**	**2×2×5**
Echo time/ repetition time [ms]	**68/2000**	**1.2/1500**	**1.21/392**
Acceleration factor (GRAPPA)	**3**	**2**	**2**
Bandwidth [Hz/pixel]	**1040**	**1085**	**1202**
Readout segments	**5**	**-**	**-**
Echo Spacing [ms]	**0.69**	**2.7**	**2.9**
Inversion Scheme	**-**	**3(3)3(3)5**	**-**
Starting TI [ms]	**-**	**117**	**-**
TI Increment [ms]	**-**	**80**	**-**
Flip Angle [°]	**180**	**35**	**12**
b-values [s/mm^2]	**0, 50, 100, 150, 200, 250, 300, 500, 700, 900**	**-**	**-**
Diffusion gradient scheme	**Bipolar**	**-**	**-**
Respiratory gating	**Belt**	**Belt**	**Breath hold**

427 **Table 2: Baseline characteristics of the study population (n = 164): clinical parameters,**

428 **medication, laboratory measurements, biopsy diagnosis and chronic histological lesions.**

Characteristics	Total (n=164)	Native (n=46)	Allograft(n=118)
Clinical parameters			
Age, years	54 ± 14	51 ± 16	55 ± 13
Male, n (%)	110 (67.1)	33 (71.7)	77 (65.3)
Body mass index, kg/m^2 (n=124)	25.7 ± 4.0	25.9 ± 4.1	25.6 ± 4.0
Caucasian, n (%)	149 (90.9)	39 (84.8)	110 (93.2)
Histological lesions			
Fibrosis in %	27.2 ± 17.7	33.3±24.1	24.9 ± 14.0
BANFF score			
IF/TA (ci+ct), min 0 – max 6 (n=116)	-	-	2 (2.0-4.0)
Medication, n (%)			
ACEi/ARB	71 (44.6)	28 (60.9)	43 (36.4)
Calcium channel blockers	66 (40.2)	14 (30.4)	52 (44.1)
Diuretics	22 (13.4)	14 (30.4)	8 (6.8)
Beta-blockers	66 (40.2)	12 (26.1)	54 (45.8)
Statins	76 (46.3)	21 (45.7)	55 (46.6)
Calcium supplementation	77 (47.0)	8 (17.4)	69 (68.5)
1.25OH-vitamin D supplementation	12 (7.3)	0 (0)	12 (10.2)
25OH-vitamin D supplementation	109 (66.5)	16 (34.8)	93 (78.8)
Anticalcineurin	-	-	111 (94.1)
Mycophenolate mofetil	-	-	94 (79.7)
Corticosteroids	-	-	85 (72.0)
Others (Azathioprine, m-Tor inhibitor, …)	-	-	11 (9.3)
Laboratory measurements			
Creatinine, micromol/l	119 [96 – 152]	120 [81-187]	119 [101-147]
eGFR ml/min per 1.73m^2 *	57.2 ± 24.2	59.2 ± 33.7	56.4± 19.4
Hemoglobin, g/l	128.6 ± 18.3	124.7 ± 23.1	130.1 ± 15.9
Calcium, mmol/l (n=142)	2.4 ± 0.1	2.3 ± 0.1	2.4 ± 0.1
Phosphate, mmol/l (n=153)	1.01 ± 0.25	1.12 ± 0.34	0.98 ± 0.21
Magnesium, mmol/l (n=118)	0.68 ± 0.11	0.80 ± 0.16	0.67 ± 0.09
25-hydroxyvitamin D, nmol/l (n=135)	71.1 ± 25.7	47.3 ± 25.7	77.0 ± 22.0
Parathyroid hormone, pmol/l (n=131)	8.8 [5.6-13.0]	6.4 [4.1-8]	10.0 [6.0 ± 13.]
Albumin, g/l (n=152)	40.3 ± 4.4	38.3 ± 5.6	41.1 ± 3.7
Proteinuria/créatinine, g/g (n=144)	0.15 [0.06-0.55]	1.00 [0.21-2.58]	0.08 [0.05-0.21]
Biopsy diagnosis,** n (%)			
Rejection	13 (7.9)	-	13 (11.0)
Positive C4D			11(9.3
Tubular lesions	29 (17.7)	6 (13.0)	23 (19.5)
- Intersitial nephritis	6 (4.6)	5 (14.3)	1 (1.1)
Glomerulonephritis incl FSGS	42 (25.6)	23 (50.0)	19 (16.1)
Diabetic nephropathy	10 (6.1)	10 (21.7)	0 (0)
Vascular nephropathy	21 (12.8)	17 (37.0)	4 (3.4)
Anticalcineurin toxicity	40 (24.4)	-	32 (27.1)
Chronic allograft nephropathy	3 (1.8)	-	3 (2.5)
Others (oxalate, amyloidosis, …)	6 (3.7)	3 (6.5)	3 (2.5)

Values reported as numbers and %, mean±SD, or median with interquartile ranges, as appropriate. *eGFR (estimated Glomerular Filtration Rate) was calculated according to the Chronic Kidney Disease Epidemiology Collaboration equation. ACEi/ARB, angiotensin-converting enzyme inhibitor/angiotensin II receptor blocker. ** One biopsy may have more than one diagnosis.

Table 3: univariable and multivariable analysis

r^2 value for the multivariable analysis was 0.54. ADC: apparent diffusion coefficient [x10^6mm^2/s]; T1[ms]; eGFR: estimated glomerular filtration rate;

	Univariable models			**Multivariable model**	
	Coefficient (95%CI)	**r^2**	**p value**	**Coefficient (95%CI)**	**p value**
ΔADC	-0.09 (-0.11 to -0.06)	0.27	<0.001	-0.05 (-0.07 to -0.03)	<0.001
ΔT1	0.06 (0.05 to 0.08)	0.23	<0.001	0.03 (0.01 to 0.05)	<0.001
eGFR	-0.41 (-0.50 to -0.31)	0.30	<0.001	-0.22 (-0.32 to -0.12)	<0.001
Phosphate	29.64 (19.61 to 39.66)	0.18	<0.001	9.35 (-0.91 to 19.6)	0.074
Hemoglobin	-0.48 (-0.61 to -0.35)	0.24	<0.001	-0.09 (-0.23 to 0.04)	0.173
Calcium	-23.97 (-46.08 to -1.85)	0.02	0.034	11.40 (-9.99 to 32.80)	0.293
Albumin	-0.98 (-1.61 to -0.35)	0.03	0.003	-0.38 (-1.06 to 0.29)	0.265
Proteinuria	3.58 (1.91 to 5.25)	0.11	<0.001	1.34 (-0.23 to 2.92)	0.093

Figure legends

Figure 1: Flowchart illustrating patient recruitment

Figure 2: Representative MRI images showing ADC, T1 and T2 maps in a kidney with low (<20%, upper row), and diffuse (>60%, lower row), cortical fibrosis. Masson trichrome sections are displayed for histological comparison.

Figure 3: Correlations between MRI indices and Fibrosis and eGFR. Scatter plots of ΔADC (A), ΔT1 (B) versus IF. **Scatter** plot of ΔADC (C), and ΔT1 (D) versus eGFR. Each symbol represents one patient. The continuous line indicates least-square linear regression. ADC: apparent diffusion coefficient. Correlation coefficient (r) and significance (p) are displayed in each scatter plot.

Figure 4: Boxplot comparison of predicted fibrosis using a multivariable model containing eGFR, ΔADC and ΔT1 and histological fibrosis in four categories (<10; ≥10-<25; ≥25-<50; >50%). The horizontal bar inside each box is the median, the top and bottom of the box indicate the interquartile range, the T bars indicate the 95^{th} percentiles.

Figure 5: ROC curves of multivariable model (ΔADC, ΔT1, eGFR) in predicting fibrosis for cutoffs of 10 % (A), 25% (B), and 50% (C) AUC: Area under the Curve; ROC: Receiver Operating Characteristic.

Supplementary figure 1: Correlations between MRI indices and Fibrosis. Scatter plots of absolute cortical ADC (A), Medullary ADC (B), cortical T1 (C) and Medullary T1 (D) versus IF. The continuous line indicates least-square linear regression. ADC: apparent diffusion coefficient. Correlation coefficient (r) and significance (p) are displayed in each scatter plot.

Supplementary Figure 2: Correlations between MRI indices and fibrosis in native and allograft patients. Scatter plots of ΔADC (A), and ΔT1 (B) versus IF, in native kidney (solid circles) and kidney allograft (open circles) patients. Each symbol represents one patient.

Supplementary Figure 3: Correlations between T2 and fibrosis in native and allograft patients. Scatter plots of absolute cortical T2 (A), medullary T2 (B), ΔT2 (C), cortical T1 (E) and cortical fibrosis. Scatter plot of ΔT2 versus eGFR (D). Scatter plots of ΔT2 versus fibrosis in native versus kidney allograft kidneys (E and F). Each dot represents one patient. The continuous line indicates least-square linear regression. eGFR: estimated glomerular filtration rate Correlation coefficient (r) and significance (p) are displayed in each scatter plot.

Supplementary Figure 4: Correlations between laboratory values and fibrosis. Scatter plots of ln Creatinine (A), ln PTH (B), 25-hydoxyvitamin D (C), ln proteinuria (D), albumin (E), eGFR(F), calcium (G), phosphate (H) and hemoglobin (I) versus interstitial fibrosis. Each symbol represents one patient. The continuous line indicates least-square linear regression. Correlation coefficient (r) and significance (p) are displayed in each scatter plot.

Supplementary Figure 5: ROC curves of ΔADC in predicting fibrosis for cutoffs of 10 % (A), 25% (B), and 50% (C) AUC: Area under the Curve; ROC: Receiver Operating Characteristic.

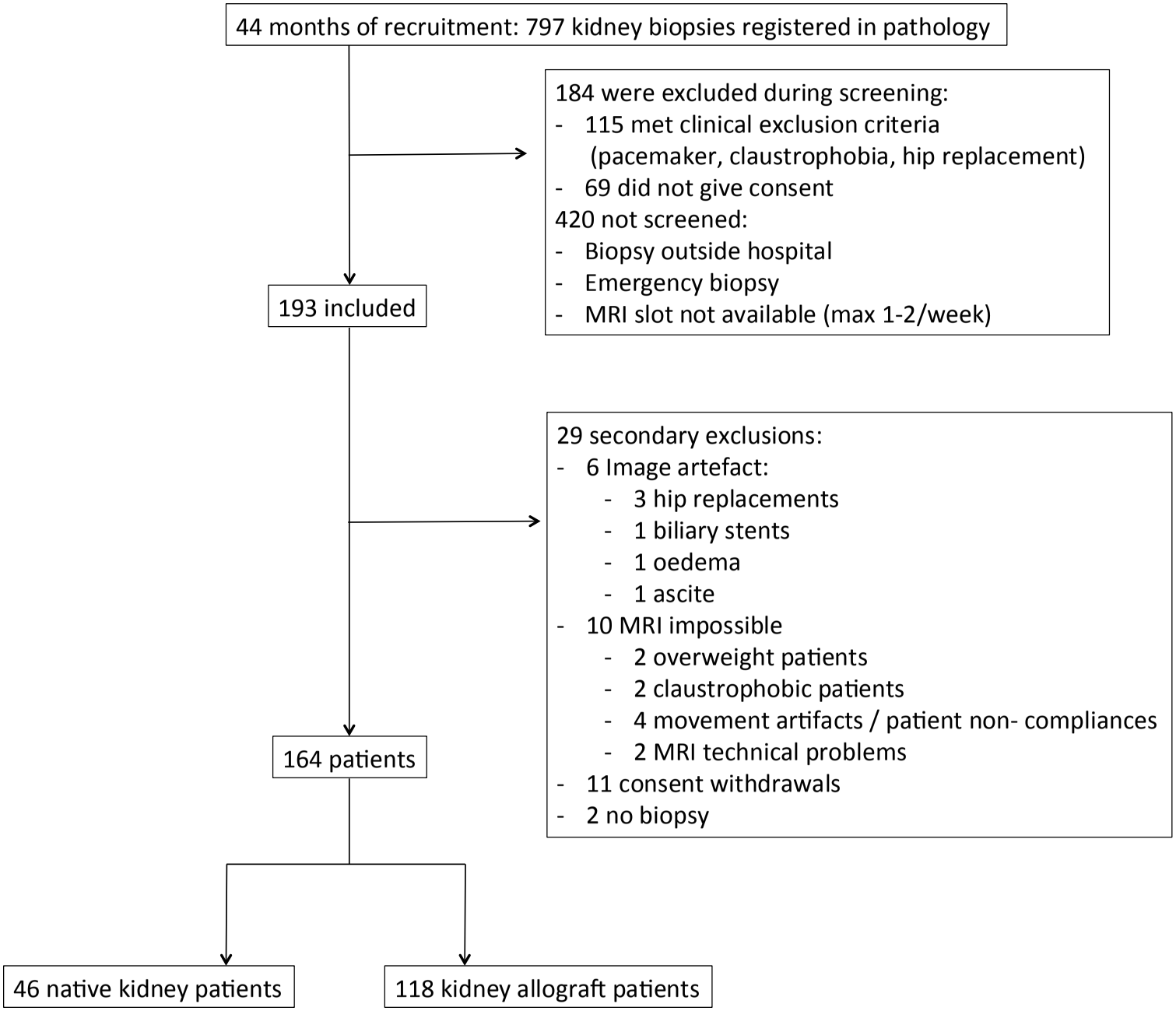
44 months of recruitment: 797 kidney biopsies registered in pathology
184 were excluded during screening:
- 115 met clinical exclusion criteria
(pacemaker, claustrophobia, hip replacement)
- 69 did not give consent
420 not screened:
- Biopsy outside hospital
- Emergency biopsy
- MRI slot not available (max 1-2/week)
193 included
29 secondary exclusions:
- 6 Image artefact:
- 3 hip replacements
- 1 biliary stents
- 1 oedema
- 1 ascite
- 10 MRI impossible
- 2 overweight patients
- 2 claustrophobic patients
- 4 movement artifacts / patient non- compliances
- 2 MRI technical problems
- 11 consent withdrawals
- 2 no biopsy
164 patients
46 native kidney patients
118 kidney allograft patients

Figure 1

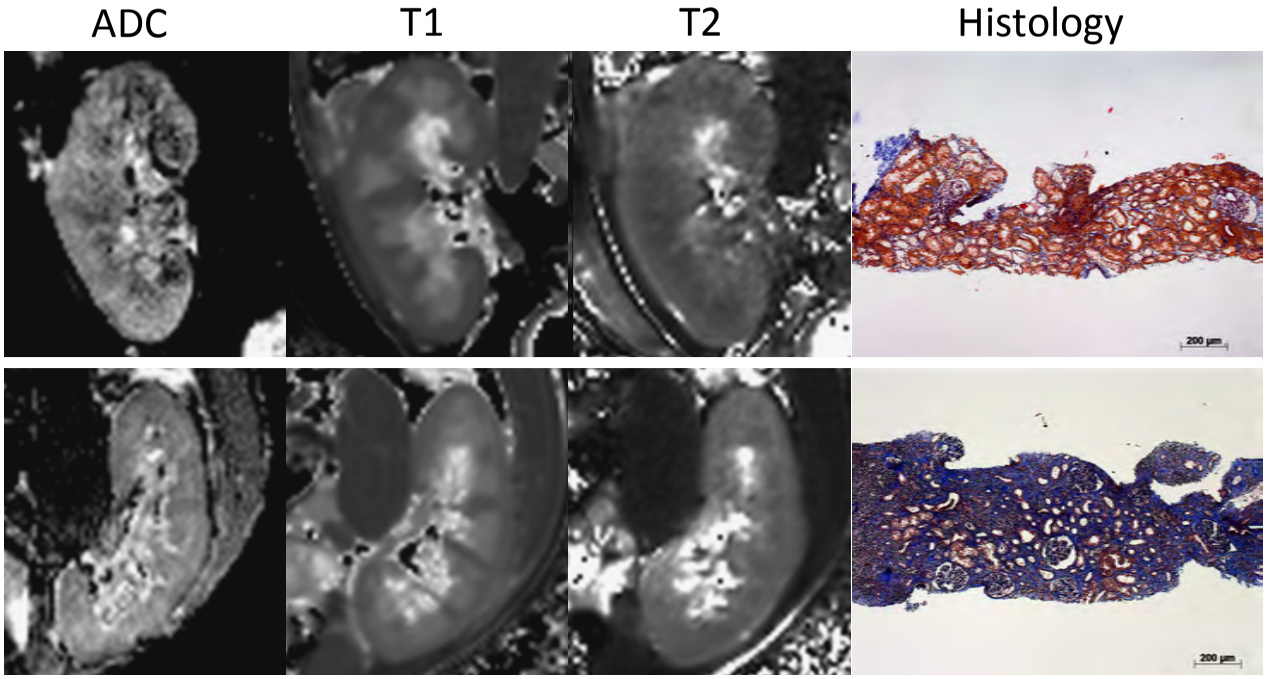

Figure 2

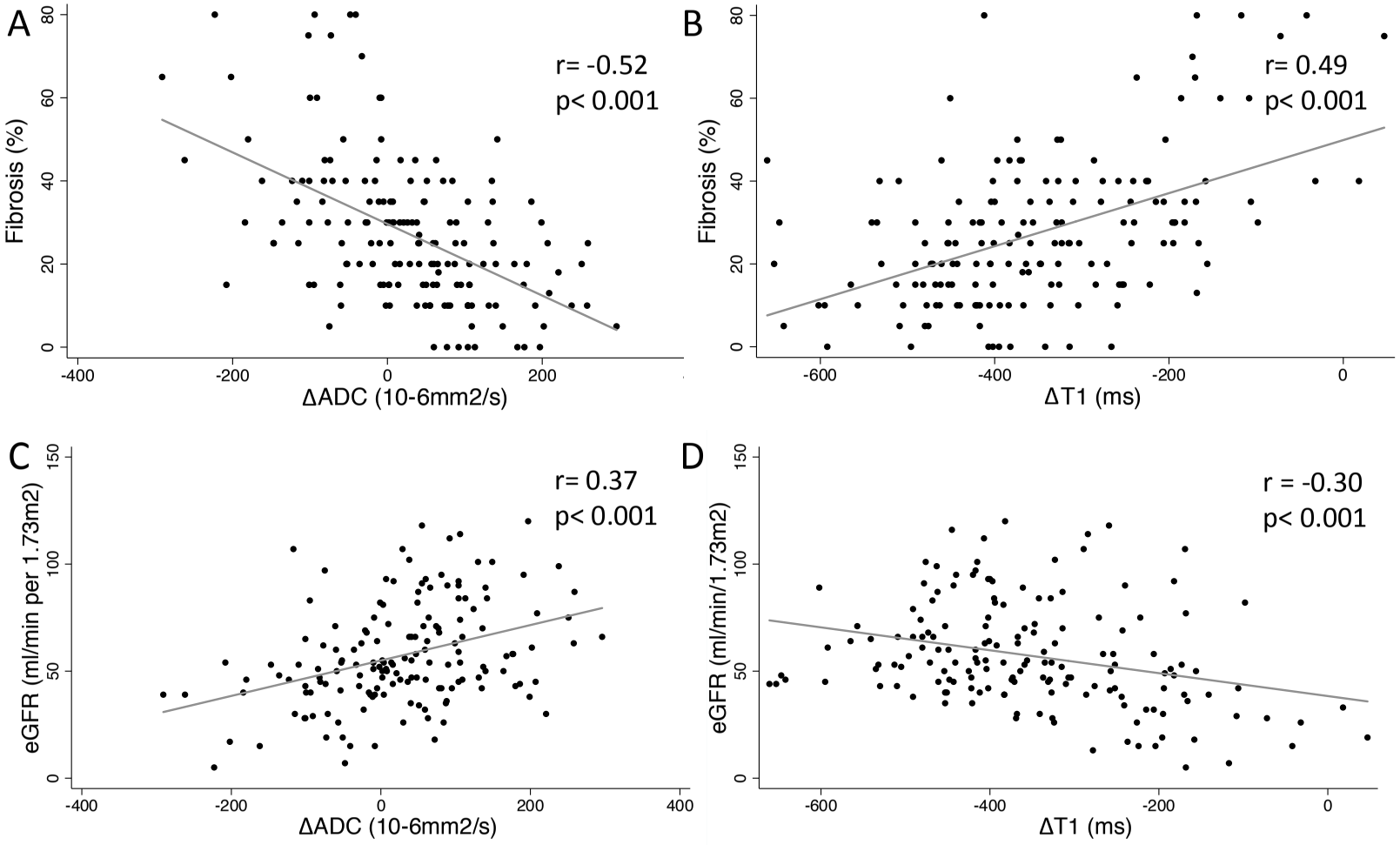
A
r= -0.52
p< 0.001
Fibrosis (%)
ΔADC (10-6mm2/s)
B
r= 0.49
p< 0.001
Fibrosis (%)
ΔT1 (ms)
C
r= 0.37
p< 0.001
eGFR (ml/min per 1.73m2)
ΔADC (10-6mm2/s)
D
r = -0.30
p< 0.001
eGFR (ml/min/1.73m2)
ΔT1 (ms)

Figure 3

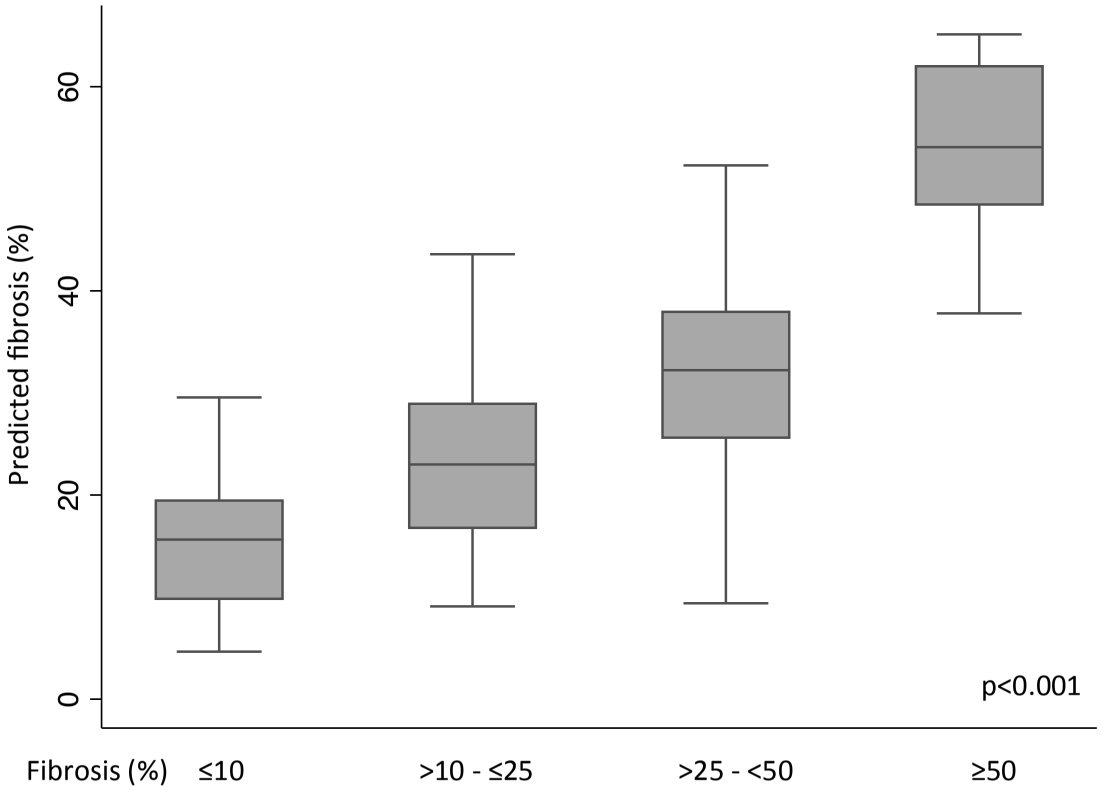

Figure 4

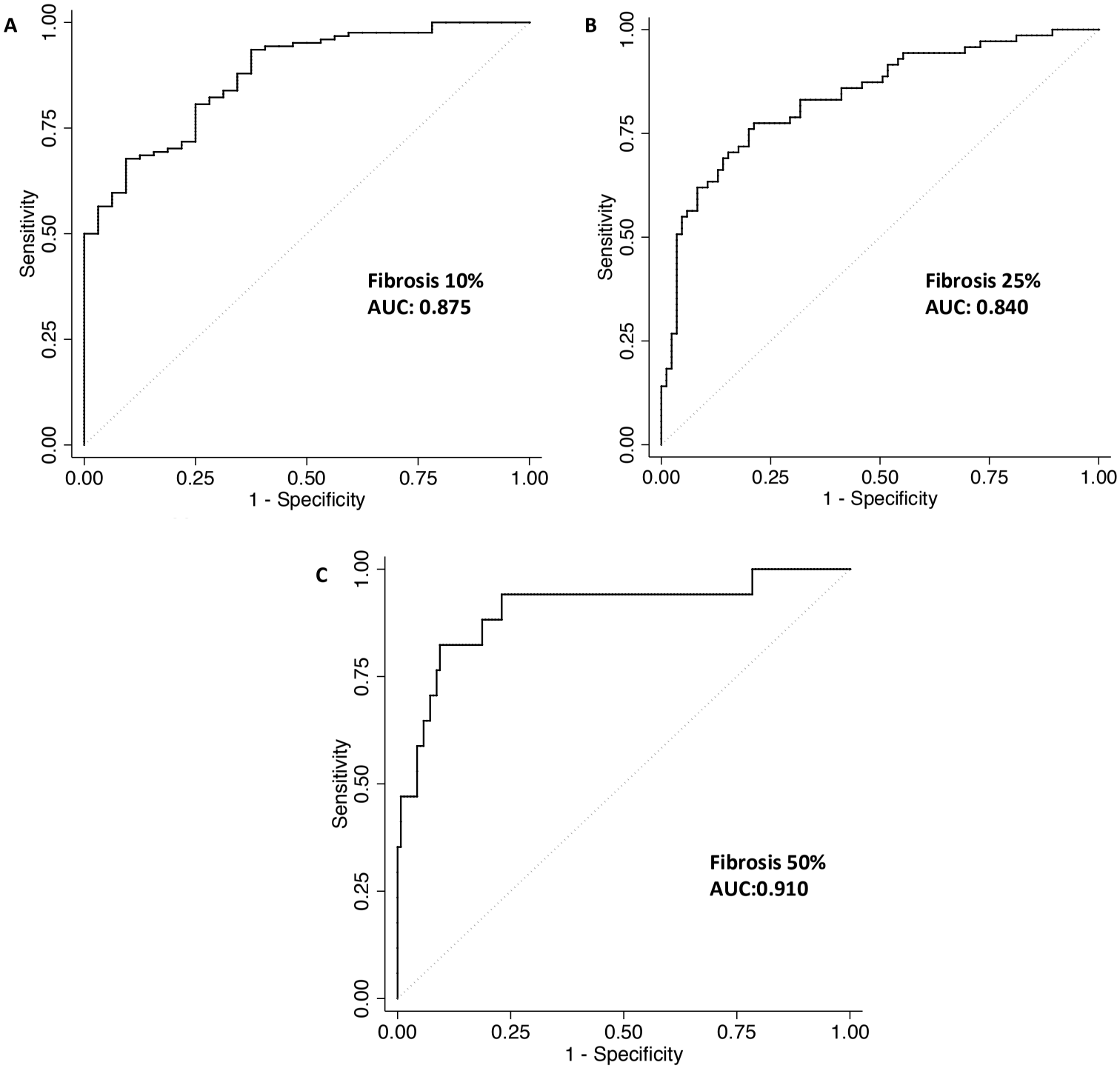
A
Sensitivity
1 - Specificity
0.00
0.25
0.50
0.75
1.00
Fibrosis 10%
AUC: 0.875
B
Sensitivity
1 - Specificity
Fibrosis 25%
AUC: 0.840
C
Sensitivity
1 - Specificity
Fibrosis 50%
AUC:0.910

Figure 5

Supplementary

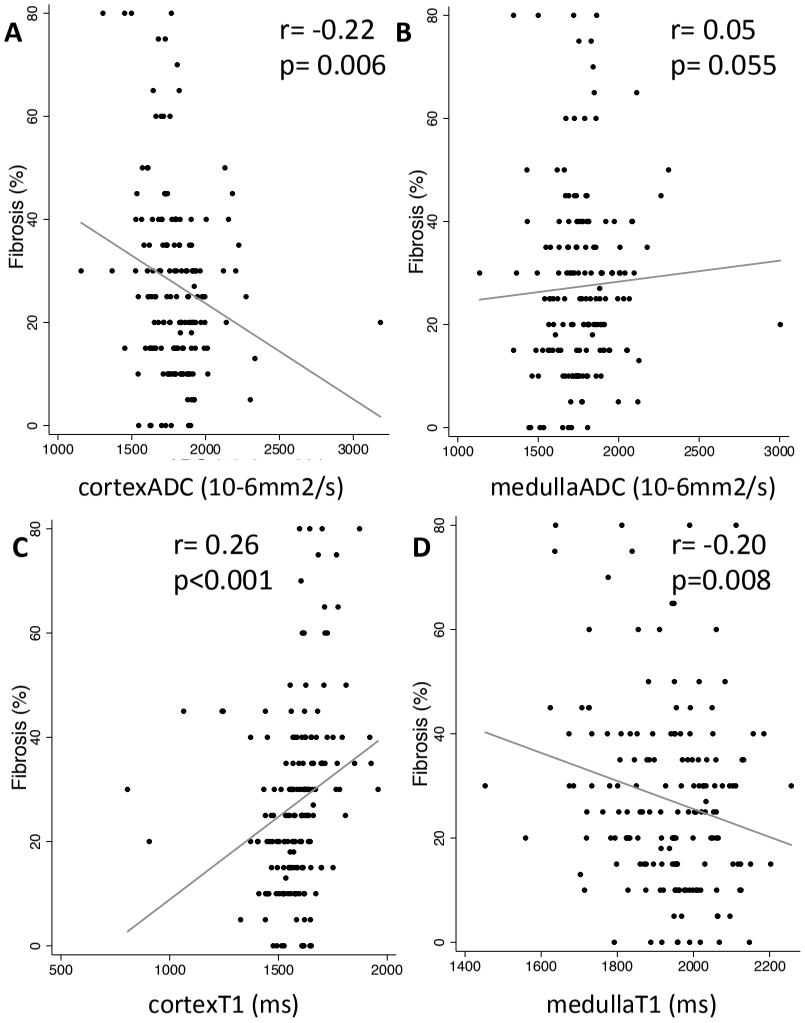

Supplementary Figure 1

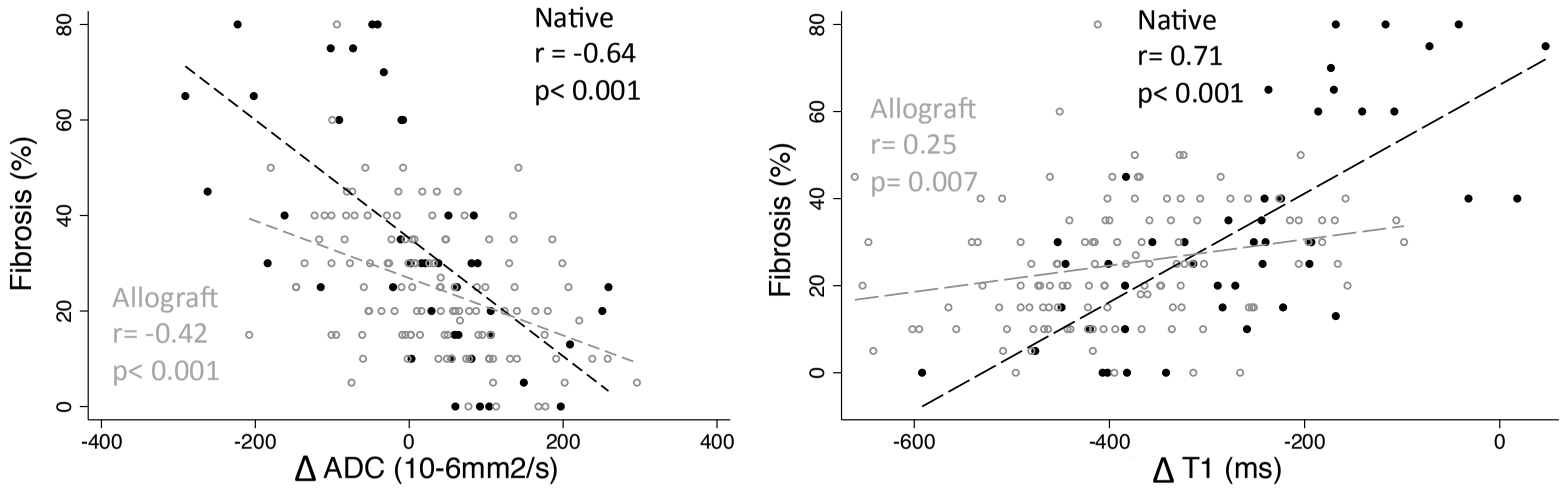

Supplementary Figure 2

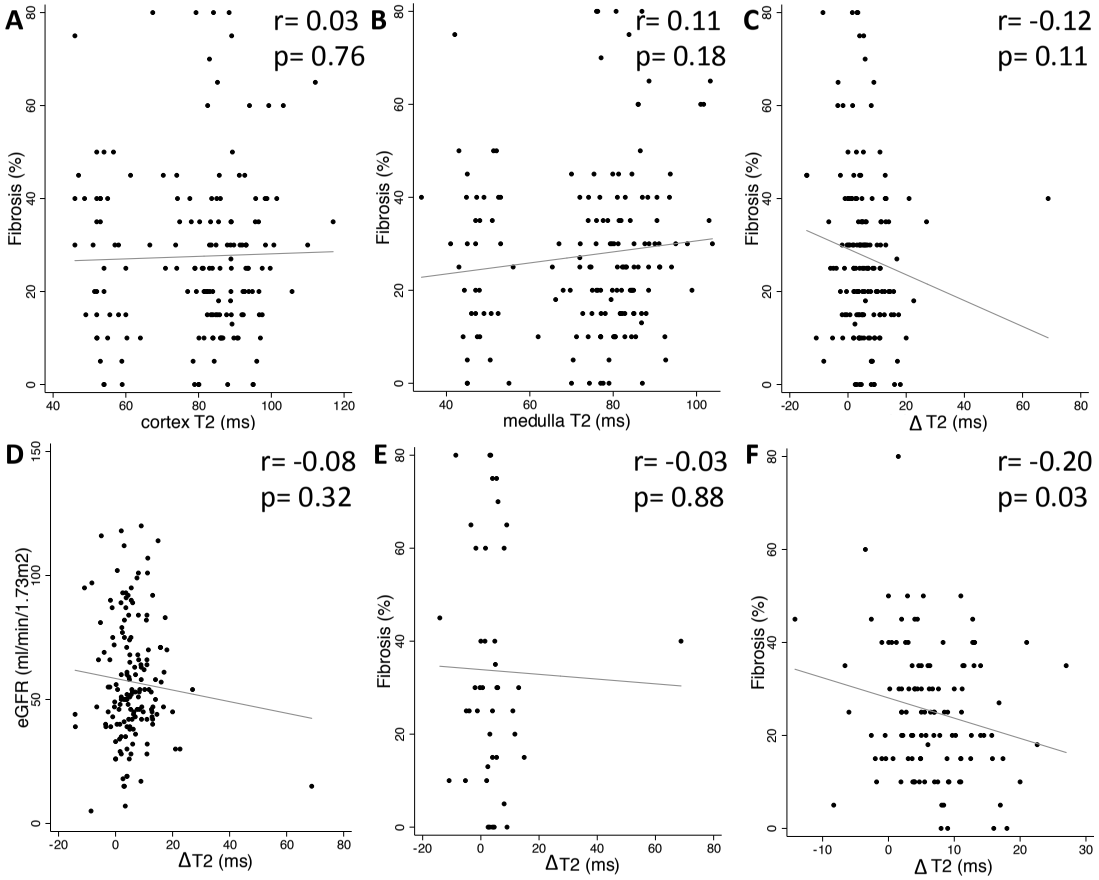

Supplementary Figure 3

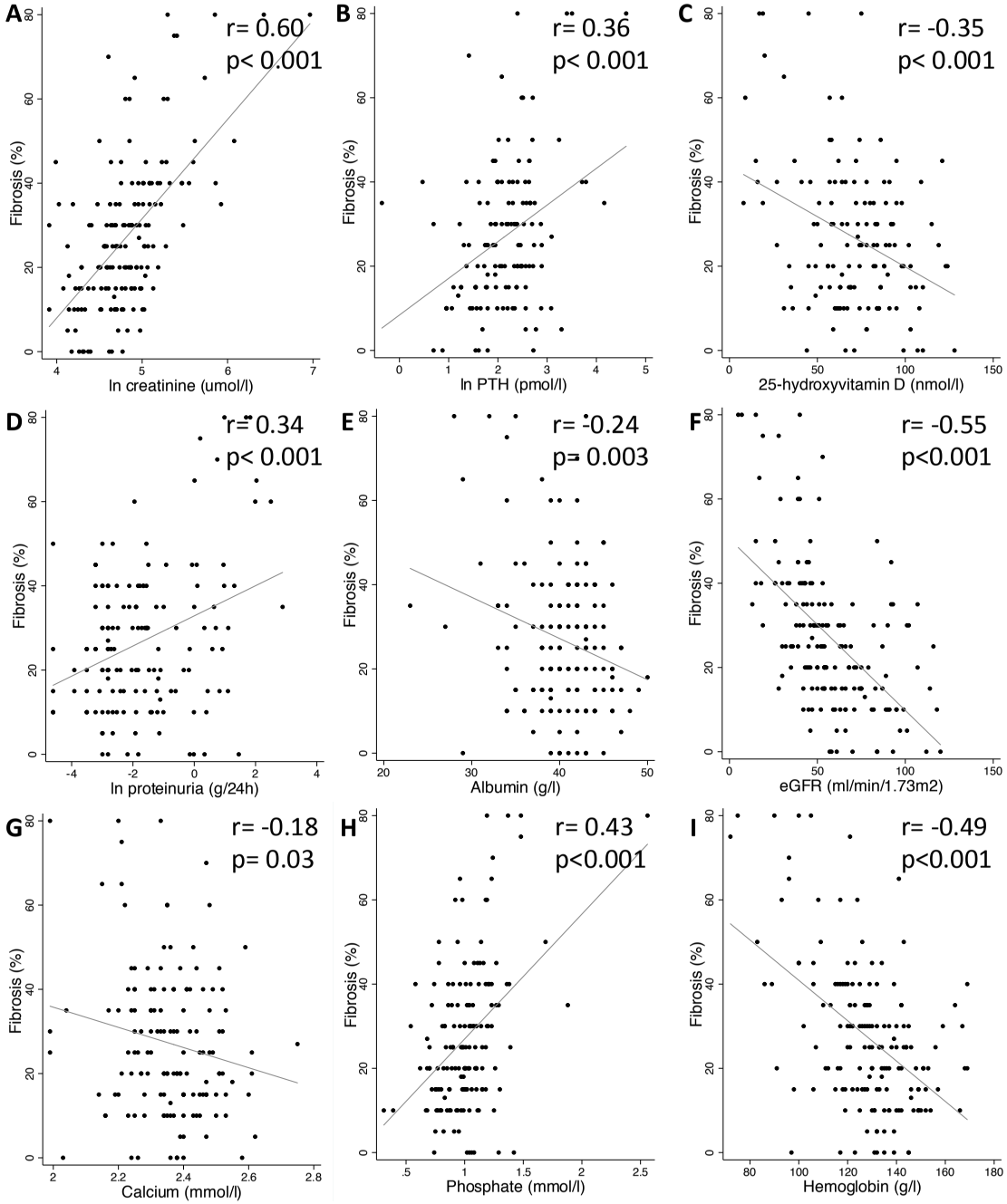

Supplementary Figure 4

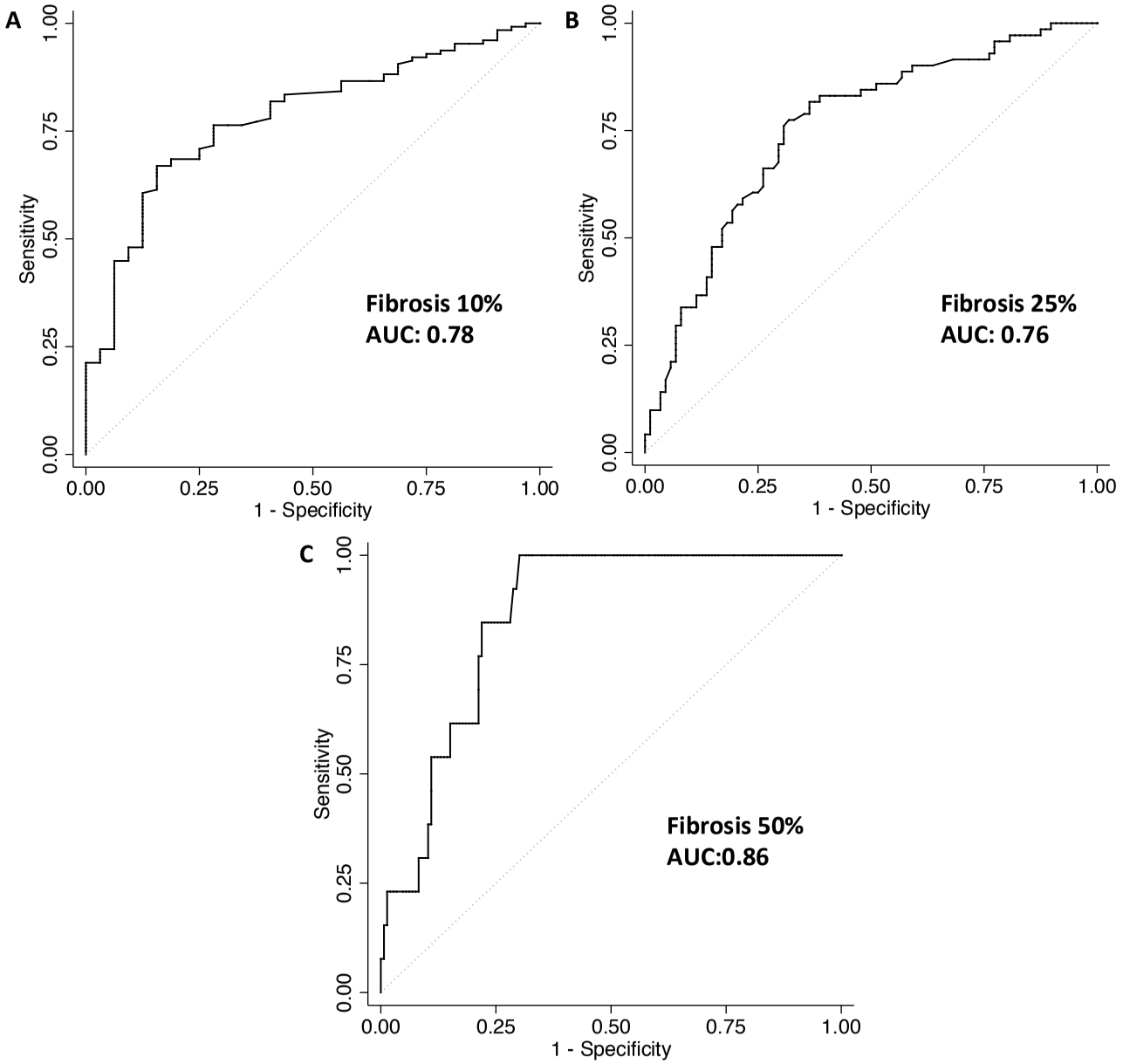

Supplementary Figure 5